Ultrafine-grained Tungsten by High-Pressure Torsion – Bulk precursor versus powder processing route

IOP Conf. Series: Materials Science and Engineering **580** (2019) 012051 doi:10.1088/1757-899X/580/1/012051

Ultrafine-grained Tungsten by High-Pressure Torsion – Bulk precursor versus powder processing route

M Wurmshuber[1,*], S Doppermann[1], S Wurster[2] and D Kiener[1]

[1] Department of Materials Science, Montanuniversität Leoben, Jahnstraße 12, 8700 Leoben, Austria
[2] Erich-Schmid Institute for Materials Science, Austrian Academy of Sciences, Jahnstraße 12, 8700 Leoben, Austria
[*] corresponding author (michael.wurmshuber@unileoben.ac.at; +43 3842 804 409)

Abstract. The continuous enhancements and developments in the field of power engineering, as well as the uprising of nuclear fusion technology, demand novel high performance materials featuring exceptional strength and damage tolerance as well as durability in harsh environments. Ultra-fine grained bulk materials fabricated by high-pressure torsion, exhibiting a grain size less than 500 nm are promising candidates for these applications. Tungsten, the material of choice for plasma-facing materials in fusion reactors, is expected to exhibit even more enhanced properties by precise doping with impurity atoms, strengthening grain boundary cohesion. In order to allow this meticulous control of chemical composition, in-house mixing of the raw material powders is preferable to use of commercially available alloys. Several challenges arise in powder processing of tungsten via high-pressure torsion, originating in the intrinsic strength and high melting point of the material, and in the affinity of the powder to oxygen. Strategies to overcome these problems will be addressed in this work. Furthermore, we compare ultra-fine grained tungsten produced from a bulk precursor to that from the developed powder approach regarding microstructural features, hardness and rate-sensitive properties. The powder route showed promising and widely comparable results to the material processed from bulk tungsten, rendering it an effective way for fabricating ultra-strong tungsten, while keeping the additional ability to accurately control chemical composition and tailor grain boundary segregation states.

1. Motivation

When it comes to implementing new ground-breaking technologies or optimizing and improving existing concepts in the sectors of power engineering, nuclear engineering, armored protection or other safety relevant applications, materials fulfilling the required standards are often the limiting factor. Ultrastrong and damage tolerant materials are of demand in these fields of application: two characteristics that are deemed mutually exclusive in many conventional materials. Nanostructured and ultra-fine grained (ufg) metals are a promising material class to combine high strength with enhanced damage tolerance [1,2], while also featuring additional beneficial properties such as radiation tolerant behavior [3,4]. While tungsten is frequently considered as candidate material for the mentioned high performance applications due to its physical properties [5–7], a rather low fracture toughness and high ductile-brittle transition temperature often impedes the utilization of tungsten-based materials. The grain boundaries are found to be one of the weak links. However, ab-initio simulations revealed that by controlling grain boundary chemistry, the grain boundary cohesion can be increased [8–10]. The consequences are repression of intercrystalline fracture, the preferred fracture mode in nanostructured materials [1,2], based on which an enhanced fracture toughness can be expected [10]. Severe plastic

deformation techniques, such as high-pressure torsion (HPT), have gained a lot of interest in recent years, as they introduce a high amount of deformation and microstructural refinement to materials, creating ultra-fine grained or nanocrystalline bulk materials. During HPT, a millimeter-sized, disk-shaped specimen is shear-deformed between two anvils under high confining pressure (several GPa). The applied von Mises-strain during HPT can be calculated using the number of rotations, the distance from the center of the disk and the thickness of the sample. Further details of the HPT process are reported elsewhere [11–13]. In order to control chemical composition precisely, a powder approach is necessary. Yet, before the chemical composition of tungsten can be altered, it must first be proven that it is possible to fabricate pure ufg tungsten with satisfactory properties from a powder starting material. Since several challenges arise with powder processing of tungsten at low temperatures using HPT, this work will address these problems and ways to mediate them. Finally, ufg tungsten samples produced from powder and a bulk precursor are compared regarding their mechanical properties.

2. Challenges with powder processing of ufg W via HPT

In order to realize systematic doping of tungsten grain boundaries, the local chemical composition of the material has to be tuned precisely. To investigate the effect of impurity atoms on the material properties thoroughly, a large number of samples with varying doping concentrations must be fabricated and characterized. Therefore, an in-house fabrication method is essential to provide a fast and easy route for processing such doped material samples, as well as to ensure access to crucial processing parameters. A powder metallurgical approach seems to be the best choice to realize this. When it comes to high-performance materials, their extraordinary properties that are desired for many of their applications often provide the biggest challenges and limitations in terms of fabrication. Tungsten is yet another example of this phenomenon, as its exceptional intrinsic strength and high melting point result in several problems that have to be tackled when processing ufg tungsten from powders on a laboratory scale. The most severe challenges that need to be handled will be addressed in this section:

2.1 Oxidation and contamination of powders

Oxidation and contamination is not only a problem for tungsten powder in particular, but for most metal powders in general. The small particle size of the powders (< 100 µm) leads to a high contact area with the surrounding atmosphere. In air and under humid conditions this can result in severe oxidation or contamination of powder particle surfaces. After processing from oxidized powder, the final components exhibit not only an oxidation layer on the surface, which could be removed rather easily, but also within the material, leading to considerable and most likely unwanted changes in material properties. Furthermore, the high hardness of metal oxides can lead to problems with compacting the powder particles or during later sintering, where oxides usually act as diffusion barriers.

In the case of W, oxidation by air already occurs at room temperature (RT). The oxidation rate accelerates significantly with increasing temperature and humidity. The oxide formed is always WO_3, which becomes volatile at temperatures above 750°C, leading to consumption of the material [6,14].

As powder oxidation has been a well known problem for decades, several solutions exist today. The most convenient one is storing and handling all powders within a so-called glovebox, a sealed container with a desired inert atmosphere (e.g. argon) inside. It is crucial that all powders are opened and manipulated inside the box using the designated gloves and that the oxygen and humidity level is kept to a minimum. For transporting the powder mixture outside of the box to the compacting facility (in this

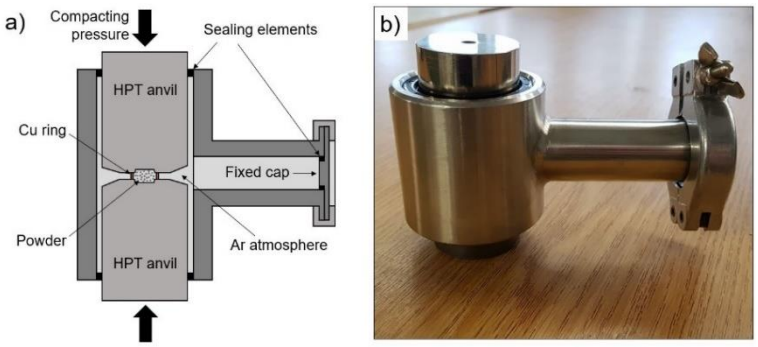

Figure 1. (a) Sketch and (b) photograph of sealed chamber to allow powder to be transported in local argon atmosphere to the HPT device.

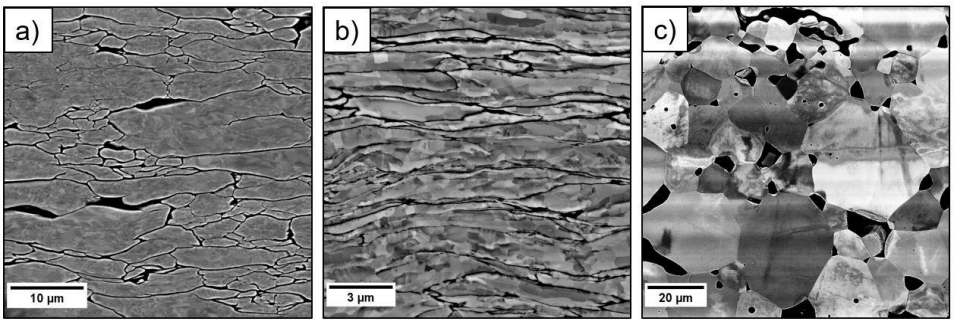

Figure 2. SEM micrographs (back-scattered mode) of (a) compacted W powder, (b) compacted and deformed W and (c) compacted and sintered W.

case the HPT tool) a small sealed container was utilized that has to be assembled together with the HPT anvils and the powder inside the glovebox (figure 1). This way the powder mixture can be transported from to the HPT tool in a local argon atmosphere and compacted without unwanted oxidation.

2.2 Compacting W powder

Due to the easy availability in the lab and the high achievable uniaxial pressures, the HPT tool can also serve as a compacting press for material powders [15,16]. The pressures reached plus a short additional shear straining is sufficient to compact the powders and close pores for most metals. Materials showing high hardness and limited ductility, such as tungsten, typically do not compact well, even under high nominal pressure. Figure 2a shows a RT compact of W powder by HPT (nominal pressure of 12 GPa). The initial powder particles changed shape due to the high pressure and applied strain, but no connection formed between the particles. The compaction is enough for the samples to be handled, but subsequent deformation by HPT will only lead to the majority of the particles shearing apart without any proper plastic deformation. The result of this deformation is a material containing lots of microcracks and pores along the initial powder particle interfaces (figure 2b). A significant improvement in interparticular bonding is expected from annealing the compacted sample, which is discussed in the next subsection.

2.3 Sintering W green compacts

Solid state sintering is a popular method to reduce porosity and increase density of powder compacted specimens of high-melting materials, such as refractory metals and ceramics. The usual temperature range for sintering is $0.6 – 0.8 * T_{melt}$ [K] [5,6]. At these elevated temperatures diffusion is enhanced, leading to a redistribution of material and closure of pores. The driving force for this process is the reduction of surface area within the material [5,6]. Conventional sintering temperatures of W are rather high (above 2000°C) due to the high melting point [5,6]. Furthermore, sintering has to be performed either in a reducing gas atmosphere or in vacuum, as oxidation is a serious problem at these temperatures.

In this work, a vacuum furnace with a maximum operating temperature of 1600°C was used for sintering the compacted tungsten samples. The microstructure after sintering is displayed in figure 2c. Naturally, the sintering process leads to substantial amount of grain growth, but this should be of no concern, as the subsequent HPT step will re-introduce grain refinement. There is still a large amount of porosity present due to the comparably low sintering temperature and the absence of any pressure applied to the material. However, it is evident that the particles have merged together and formed large grains. Therefore, severe plastic deformation applied during HPT should be able to close the residual pores and deform the material sufficiently to reduce the grain size to the ufg regime. In general, it is beneficial to work with relatively small powders (< 10 µm), as they show enhanced surface diffusion, improving the densification by sintering considerably.

2.4 Severe plastic deformation of W

While all the limitations from a powder starting material can be handled by adapting the approaches described in the previous subsections, HPT processing of pure W, even from a bulk precursor, is not a straightforward task. High strength, low ductility and the high melting point are again an issue when it comes to severe plastic deformation of tungsten. The presence of dislocation plasticity is advantageous in order to allow the necessary deformation and grain refinement [13]. For tungsten, a body-centered cubic (BCC) metal, dislocation plasticity is fully thermally activated at ~ 460°C ($0.2 * T_{melt}$ [K]) [17,18].

On the contrary, in order to deform a material using HPT, the hardness of the anvils (~850 HV; tool steel Böhler S390) has to be somewhat higher than the sample [12]. Heating to a temperature above 400°C leads to considerable softening of the anvils. Therefore, a trade-off in deformation temperature is necessary to find the ideal conditions for severe plastic deformation of W. Increasing the applied nominal pressure by decreasing the sample radius also results in better deformability of tungsten.

Even by considering all these aspects, the maximum number of rotations possible by HPT in this work did not exceed 1.5 turns, the equivalent of ~1800 % strain, as the material becomes too hard from grain refinement to be further processed by the available anvils.

3. Fabrication route for ufg W from powders

The raw tungsten powder (particle size 2 µm, purity 99.97%) provided by Plansee SE was opened, stored and handled only in argon atmosphere within a glovebox (M. Braun LABstar Glove Box Workstation). A copper ring is glued around the cavity of the HPT anvil (diameter 6 mm, depth 0.15 mm) to allow more powder to be filled in the cavity without spilling. Subsequently, the sealed mini-chamber is assembled around the powder filled anvil and its counterpart within the glovebox (figure 1). The chamber is then inserted in a HPT tool [12] and the powder sample is compacted under a pressure of 12 GPa and deformed for 30-40 seconds at a speed of 0.2 rpm. Afterwards, the mini-chamber is opened and the residual copper around the sample removed. Subsequently, the compacted sample is annealed in a vacuum furnace (Leybold Heraeus PD 1000) at 1600°C for 7 hours at a pressure lower than 10^{-4} mbar. In addition, HPT samples have been manufactured from ultra-high purity tungsten bulk material (99.9999% purity, Plansee SE). The material disks were deformed using the HPT tool with a pressure of 12 GPa at 300°C and 400°C for the maximum amount of turns possible (1 – 1.5 turns).

4. Material characterization

After processing, the microstructure of all samples was investigated in the tangential direction using a field-emission scanning electron microscope (SEM; LEO type 1525). Vickers microhardness was measured along the radius with a load of 500 g (HV0.5) using a Buehler Micromet 5104 machine. Nanoindentation tests were performed with a KLA G200 Nanoindenter using a Berkovich tip and the continuous stiffness measurement (CSM) method [19,20]. Strain rate jump tests [21,22] were conducted with the same nanoindentation setup to investigate strain rate sensitivity and activation volume.

5. Results and discussion

5.1 Microstructure

Micrographs of all materials at a radius of 3 mm (outer edge of the HPT deformed disk, corresponding to strains of ~ 10-17) were recorded using the SEM in backscattered electron mode and are displayed in figure 3. It is apparent from the micrographs that both bulk and powder processed materials exhibit a similar microstructure and grain sizes of ~110-160 nm for each deformation temperature, as detailed in table 1. No pores or oxide layers are visible in the samples fabricated from powders.

5.2 Microhardness

Microhardness testing is a fast method to assess the gradient in mechanical properties in HPT deformed materials to check whether the deformation was high enough to reach the saturation state, i.e. the point where grain size cannot be refined any further due to a dynamic equilibrium of dislocation generation

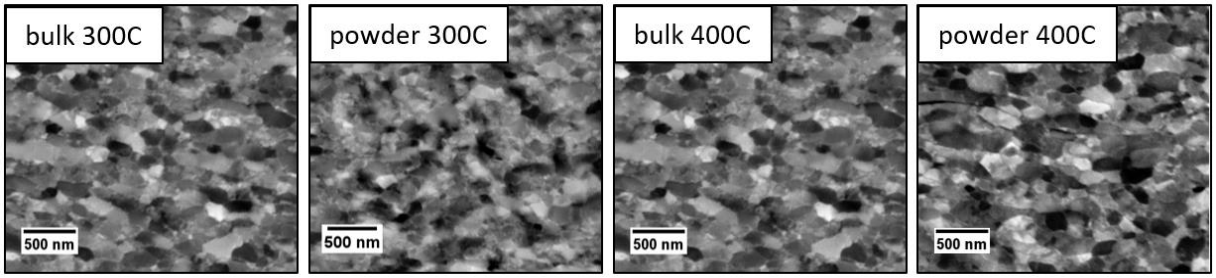

Figure 3. SEM images (backscattered electron mode, same magnification for all images) of resulting microstructures of bulk and powder processed samples after HPT deformation at different temperatures.

Table 1. Results from microstructural evaluation, microhardness and nanoindentation tests. If not stated otherwise, the values were measured at a radius of 3 mm on the sample disk.

Deformation temperature	300°C		400°C	
Precursor	bulk	powder	bulk	powder
Grain size @ 3 mm [nm]	112 ± 19	127 ± 25	143 ± 26	158 ± 36
Grain size @ 1 mm [nm]	173 ± 39	163 ± 46	219 ± 66	256 ± 78
Microhardness [HV0.5]	884	940	871	850
Nanohardness [GPa]	11.17 ± 0.28	11.02 ± 0.16	10.27 ± 0.08	9.96 ± 0.56
Elastic modulus [GPa]	394 ± 8	410 ± 4	402 ± 4	408 ± 16
Strain rate sensitivity [-]	0.016 ± 0.002	0.017 ± 0.002	0.016 ± 0.002	0.015 ± 0.002
Activation volume [b³]	6.78 ± 0.89	6.21 ± 0.69	7.22 ± 0.99	7.59 ± 0.82

and annihilation [13]. The trend of measured microhardness with applied von Mises-strain for all material samples is displayed in figure 4a. All samples could be deformed for between 1 and 1.5 turns, corresponding to strains of ~10-17. One can observe that the hardness is still increasing at the highest achieved strains, indicating that the saturation regime was not reached for any material and deformation temperature. The hardness gradient over applied strain for both samples deformed at 400°C and for the powder sample deformed at 300°C are in good agreement. The bulk sample deformed at 300°C shows a higher hardness for low strains, which could be due to possible differences in the initial microstructure. At high strains, this sample shows a similar hardness trend as all other samples.

To allow a better correlation with the mechanical properties gained from microhardness tests, the grain sizes were evaluated at a radius of 1 mm and 3 mm using the grain intercept method (see table 1). When plotting the hardness versus the inverse square root of the grain size (figure 4b), one can see that all materials follow a clear linear trend in accordance with the Hall-Petch relationship [23,24]. The slope of the Hall-Petch line k_y = 8.7 kg/mm$^{-3/2}$ is found to be in good agreement with literature (10 kg/mm$^{-3/2}$) [25]. Serious contamination or residual pores in the powder processed material should have led to a pronounced deviation from the Hall-Petch behavior of the bulk samples. This is an important finding, as it proves that by adapting the enhancements to the powder processing route presented in Section 2, the successful fabrication of ufg W with nanostructured grains and a comparable hardness-microstructure relationship than processed from bulk precursor material is possible.

5.3 Nanoindentation tests

Nanoindentation provides a locally resolved evaluation of both plastic (hardness) and elastic (modulus) properties of a material. By superimposing a sinusoidal signal on the conventional load signal, a continuous evaluation of hardness and modulus with indentation depth is possible (CSM method) [20]. The results from CSM nanoindentation tests are displayed in table 1. All samples were indented at least 6 times at a radius of 3 mm, where the finest grain size and highest hardness values are present. The hardness values from nanoindentation were found to be ~10 – 11 GPa. The measured elastic moduli lie in the range for the modulus of tungsten reported in literature of 390 – 410 GPa [6,26]. Body-centered

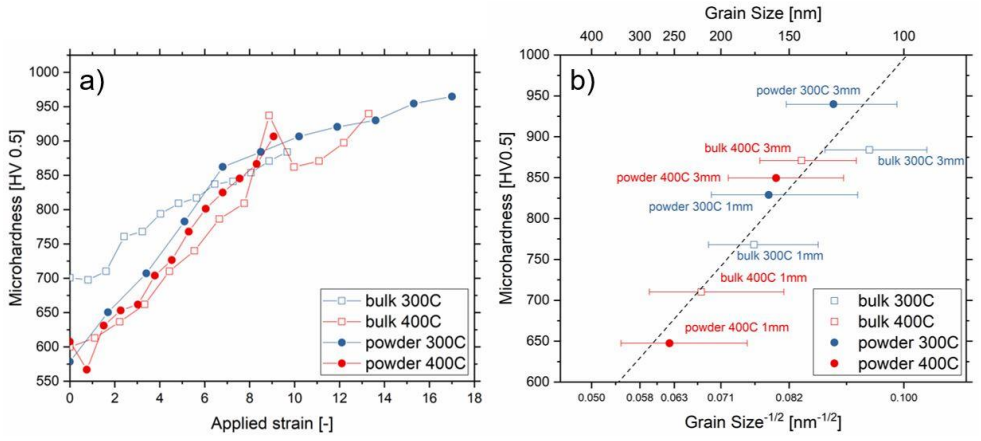

Figure 4. (a) Microhardness progression with applied HPT strain. (b) Hall-Petch plot of bulk and powder processed samples.

cubic and ultra-fine grained metals exhibit different mechanical properties dependent on the strain rate they are loaded with, a phenomenon known as strain-rate sensitivity (SRS) [27]. The origin of this material behavior is believed to lie in the intrinsic deformation behavior of the BCC lattice and the increased amount of dislocation-grain boundary interactions [27]. Dislocation pinning by impurites can also have a significant influence on the SRS. The SRS exponent and the activation volume for plastic deformation can be obtained from nanoindentation strain rate jump tests [21,22].

Calculated values of the SRS and activation volume obtained from strain-rate jump tests for each sample are given in table 1. All samples show similar dependence on strain rate, indicating the same deformation mechanisms in all tested materials. Moreover, the similar values of SRS suggest that the powder processed samples do not exhibit a significantly increased amount of impurities compared to the samples processed from bulk W. The magnitude of the measured activation volume (around 7 b^3) lies in the regime of grain boundary-dislocation interactions [1,21,27]. However, as previous experiments on single crystalline and ufg W have reveiled, this value for activation volume corresponds also to the activation energy for the kink-pair mechanism, which is believed to be the dominant deformation mechanism for this material and testing temperature [18].

6. Summary and outlook

In conclusion, we established a powder processing route for ufg W resulting in similar microstructural evolution, mechanical properties, deformation behavior and microstrucure-property relationships as ufg W fabricated from a bulk starting material. Although the powder processing route is more time-consuming, the ability to control chemical composition in terms of precise doping with impurity or alloying elements clearly underlines its benefits. The developed fabrication route can now be used to tune grain boundary segregation states and explore the effect of doping of grain boundaries in ufg W on the investigated properties and on fracture behavior and performance in harsh environments, with the goal of fabricating novel high-performance materials for application in future engineering technologies.

Acknowledgements

The authors acknowledge funding by the European Research Council under Grant number: 771146 (TOUGHIT). Financial support under the scope of the COMET program (A2.12) within the K2 Center “IC-MPPE” (Project No 859480) is gratefully acknowledged.

References

[1] Meyers M A, Mishra A and Benson D J 2006 *Prog. Mater. Sci.* **51** 427–556
[2] Hohenwarter A and Pippan R 2015 *Philos. Trans. R. Soc. A*
[3] Wurster S and Pippan R 2009 *Scr. Mater.* **60** 1083–7
[4] Wurmshuber M, Frazer D, Bachmaier A, Wang Y, Hosemann P and Kiener D 2018 *Mater. Des.* **160** 1148–57
[5] Pink E and Bartha L 1989 *The metallurgy of doped/non-sag tungsten* (Essex: Elsevier Science Publishers Ltd)
[6] Lassner E and Schubert W-D 1999 *Tungsten. Properties, Chemistry, Technology of the Element, Alloys, and Chemical Compounds* (New York: Kluwer Academic / Plenum Publishers)
[7] Neu R, Dux R, Kallenbach A, Pütterich T, Balden M, Fuchs J C, Herrmann A, Maggi C F et al. 2005 *Nucl. Fusion* **45** 209–18
[8] Scheiber D, Pippan R, Puschnig P and Romaner L 2016 *Model. Simul. Mater. Sci. Eng.* **24** 85009
[9] Scheiber D, Pippan R, Puschnig P, Ruban A and Romaner L 2016 *Int. J. Refract. Met. Hard Mater.* **60** 75–81
[10] Leitner K, Scheiber D, Jakob S, Primig S, Clemens H, Povoden-Karadeniz E and Romaner L 2018 *Mater. Des.* **142** 36–43
[11] Valiev R Z, Islamgaliev R K and Alexandrov I V. 2000 *Prog. Mater. Sci.* **45** 103–89
[12] Pippan R, Scheriau S, Hohenwarter A and Hafok M 2008 *Mater. Sci. Forum* **584**–**586** 16–21
[13] Pippan R, Scheriau S, Taylor A, Hafok M, Hohenwarter A and Bachmaier A 2010 *Annu. Rev. Mater. Res.* **40** 319–43
[14] Warren A, Nylund A and Olefjord I 1996 *Int. J. Refract. Met. Hard Mater.* **14** 345–53
[15] Zhilyaev A P and Langdon T G 2008 *Prog. Mater. Sci.* **53** 893–979
[16] Bachmaier A and Pippan R 2013 *Int. Mater. Rev.* **58** 41–62
[17] Kraft O and Arzt E 2009 *Phys. Rev. Lett.* **103** 105501
[18] Kiener D, Fritz R, Alfreider M, Leitner A, Pippan R and Maier-Kiener V 2019 *Acta Mater.* **166** 687–701
[19] Pharr G M and Oliver W C 1992 *J. Mater. Res.* **7** 1564–83
[20] Hay J, Agee P and Herbert E 2010 *Exp. Tech.* **34** 86–94
[21] Maier-Kiener V and Durst K 2017 *Jom* **69** 2246–55
[22] Maier V, Durst K, Mueller J, Backes B, Höppel H W and Göken M 2011 *J. Mater. Res.* **26** 1421–30
[23] Hall E O 1951 *Proc. Phys. Soc.* **64** 747–53
[24] Petch N J 1953 *J. Iron Steel Inst.* **174** 25–8
[25] Vashi U K, Armstrong R W and Zima G E 1970 Powder *Met. Trans.* **1** 1769–71
[26] Grünwald E, Nuster R, Treml R, Kiener D, Paltauf G and Brunner R 2015 *Mater. Today Proc.* **2** 4289–94
[27] Caillard D and Martin J L 2003 *Thermally activated mechanisms in crystal plasticity* (Kidlington: Elsevier Ltd.)